


RIV000103
Submitted: June 19, 2012

*International Conf. on Liquid Metal Technology
May 3-6, 1976, Champion, PA.*

CONF-760503-19

United States Nuclear Regulatory Commission Official Hearing Exhibit	
In the Matter of:	Entergy Nuclear Operations, Inc. (Indian Point Nuclear Generating Units 2 and 3)
	ASLBP #: 07-858-03-LR-BD01
	Docket #: 05000247 05000286
	Exhibit #: RIV000103-00-BD01
	Admitted: 10/15/2012
	Other:
	Identified: 10/15/2012
	Withdrawn:
	Stricken:

SMALL SODIUM-TO-GAS LEAK BEHAVIOR IN RELATION
TO LMFBR LEAK DETECTION SYSTEM DESIGN

J. Hopfenfeld, G. R. Taylor, and L. A. James

NOTICE
This report was prepared as an account of work sponsored by the United States Government. Neither the United States nor the United States Energy Research and Development Administration, nor any of their employees, nor any of their contractors, subcontractors, or their employees, makes any warranty, express or implied, or assumes any legal liability or responsibility for the accuracy, completeness or usefulness of any information, apparatus, product or process disclosed, or represents that its use would not infringe privately owned rights.

MASTER

28
DISTRIBUTION STATEMENT
CONTRACT NO. AT(11-1)-3045

ABSTRACT

This paper discusses various aspects of sodium-to-gas leaks which must be considered in the design of leak detection systems for LMFBR's. Attention is focused primarily on small weeping type leaks. Corrosion rates of steels in fused sodium hydroxide and corrosion damage observed at the site of small leaks lead to the conclusion that the sodium-gas reaction products could attack the primary hot leg piping at rates up to 0.08 mils per hour. Based on theoretical considerations of the corrosion mechanism and on visual observations of pipe topography following small sodium leak tests, it is concluded that pipe damage will be manifested by the formation of small detectable leaks prior to the appearance of larger leaks. The case for uniform pipe corrosion along the pipe circumference or along a vertical section of the pipe is also examined. Using a theoretical model for the gravity flow of sodium and reaction products along the pipe surface and a mass transport controlled corrosion process, it is shown that below sodium leak rates of about 30 g/hr for the primary piping corrosion damage will not extend beyond one radius distance from the leak site.

A method of estimating the time delay between the initiation of such leaks and the development of a larger leak due to increased pipe stresses resulting from corrosion is presented.

INTRODUCTION

The design of LMFBR sodium-to-gas leak detection systems requires reliable information regarding leak size and instrument response time because these factors influence detector selection with respect to sensitivity, reliability and location in the system. The requirement for a leak detection system is dictated by the objective of minimizing forced outage as a result of sodium-to-gas leaks.

Although a leak detection system cannot prevent the occurrence of leaks it can, when properly designed, detect leaks which if they proceeded undetected might result in significant down time to the plant.

From the data given in Reference 1 it can be shown that one day downtime of a 1000 MW plant incurs a loss of 700,000 to 1,000,000 dollars, and therefore the capital cost of a leak detection system compared to its potential benefits is very small indeed. To maximize these benefits, the leak detection system must be capable of detecting leaks "as small as possible and practical" and at the same time be completely free of spurious behavior. However, since an increase in system sensitivity to leak size will generally be accompanied by the vulnerability of the leak detection system to false signal generation, the judicious selection of the smallest leak size that must be detected assumes paramount importance.

During the past two years, ERDA has sponsored a series of studies on leak initiation and leak behavior in order to provide a sound rationale for the assessment of LMFBR pipe integrity and the design of leak detection systems. These studies examined the (a) self-plugging of small sodium leaks; (b) material wastage in areas adjacent to small sodium leaks; and, (c) fatigue crack propagation with and without the presence of sodium leaks.

A detailed description of the above programs can be found in References 2, 3, and 4.

The purpose of this paper is to elucidate how the results of these studies relate to the establishment of instrumentation requirements for the detection of sodium to gas leaks. The discussion below starts with a description of the various aspects of sodium leaks.

Hydraulic Aspects of Sodium Leaks

The flow of sodium through a crack in the pipe wall and its flow on or away from the pipe surface depends on factors such as temperature, pressure,

concentration of oxygen and water vapor in the gaseous environment, crack size and geometry and the general piping arrangement in the cell. The flow through the crack can be approximated by the equation for laminar flow of a viscous liquid in a channel of elliptical flow cross-section(5).

$$Q = \frac{\pi(a^3b^3)}{4(a^2+b^2)} \cdot \frac{\Delta P}{\mu l} \quad (1)$$

where

- Q = volumetric flow rate
- 2a = major axis of ellipse
- 2b = minor axis of ellipse
- ΔP = pressure drop
- l = length of flow path
- μ = fluid viscosity.

For small cracks in pipes, the crack length (2a) is generally very much larger than the width (2b), so that $a^3b^3/(a^2+b^2) = a b^3$. Also the crack width is related to the stress, and thus the pipe diameter and internal pressure by(6)

$$b = \frac{ca}{2E\beta} \ln \left(\frac{\sin \beta + 1}{\sin \beta - 1} \right)^2 \quad (2)$$

where

- σ = the tension stress normal to the crack
- E = Young's modulus
- $\beta = \frac{\pi}{2} (\sigma/Y)$
- Y = yield stress of the material

If the applied stress is sufficiently below yield, as is the case here, Equation 2 can be approximated by:

$$b = \frac{2\sigma a}{E} \quad (3)$$

Noting that $c \approx D \Delta P/2t$ for axial cracks in a pipe of diameter D and wall thickness t, Equation 1 becomes:

$$Q = \frac{\pi}{4} \cdot \frac{a^4 D^3 \Delta P^4}{E^3 \mu t^3 l} \quad (4)$$

Note that usually for pipe cracks $t = l$; however in some experimental situations a crack is formed by electric discharge machining or otherwise

forming a starter notch part way through the wall prior to fatigue cracking the specimen. In the latter case λ will be less than t by the depth of the starter notch.

On leaving the crack the sodium reacts with the surrounding atmosphere forming reaction products which are either liquids or solids. Depending on the issuing velocity of the leaking sodium and the rate of the chemical reaction to form these products, the products of reactions will be formed on the surface of the pipe in the vicinity of the leak and on the surrounding insulation, or on pipe surfaces relatively far removed from the leaking area. At relatively low leak velocities the reaction products will be formed in the neighboring areas of the crack and if in a solid form they will introduce an additional resistance in the path of the leaking sodium and reduce the leak intensity. Under these conditions, and since the solid reaction products are somewhat porous, the flow of sodium may be controlled by capillary forces within the deposit rather than by the pressure across the crack. As more and more products are accumulated near the crack the resistance to sodium flow increases, eventually causing the leak to stop. On the other hand when the sodium velocity is large, sodium will impact the pipe insulation cladding no matter where the leak is located circumferentially on the pipe. The sodium will form a liquid sheet along the insulation wall which may eventually fall back on the pipe by gravity. In this case reaction products will be formed both on the insulation and the piping in areas removed from the original leak. A quantitative distinction between leaks can be made if one chooses to employ the minimum velocity required for a leak occurring anywhere on the pipe surface to reach the insulation. This velocity is simply given by $U = \sqrt{2g\lambda}$ which for a 3" gap between the pipe and the insulation is approximately 4 ft/sec. for $\Delta p = 200$ psi, $D = 24"$, $\lambda = 3/8"$ and temperature of 1000°F the corresponding crack length from Equation 4, noting that $U = Q/\lambda b$, is 1.16 cm (0.459 in.) and the width is only 5.94 μm (1.52×10^{-3} in.). The leak rate (191 g/hr), then, per unit of crack length is approximately 164 g/hr-cm. Solid reaction products originating from leaks which are smaller than 164 g/hr-cm (on the order of 10 g/hr-cm or less) are expected to concentrate in the immediate vicinity of the leak eventually plugging the leak. Reaction products resulting from leaks larger than 164 g/hr-cm are more likely to disperse over larger areas and could plug the leak only if the annulus between the pipe and the insulation is filled with reaction products.

In an experimental measurement of sodium leak rates, plugging characteristics, and external corrosion effects^(2,3) it was found that the observed leak rate was from 3 to 24 times as large as the calculated leak rate as shown in Table 1. This discrepancy may be due to fluid slip at the wall (sodium not wetting the crack surfaces), or possibly slight distortion (yield) of the crack during the fatigue crack growth operation, or both.

In none of these tests was there any tendency for spraying (all less than 110 g/hr). In several cases the rate of formation of reaction products was sufficiently high relative to the leak rate so that solid reaction product cakes or deposits formed over and around the crack, leading in general to decreased leak rates, and in two cases to complete cessation

FIGURE 1 Typical Appearance of Sodium Reaction Products.
Leak to H_2 , 1% O_2 , 1000 ppm H_2O ; Sodium at 800°F,
after two hours, approximate leak rate, 67 g/hr.

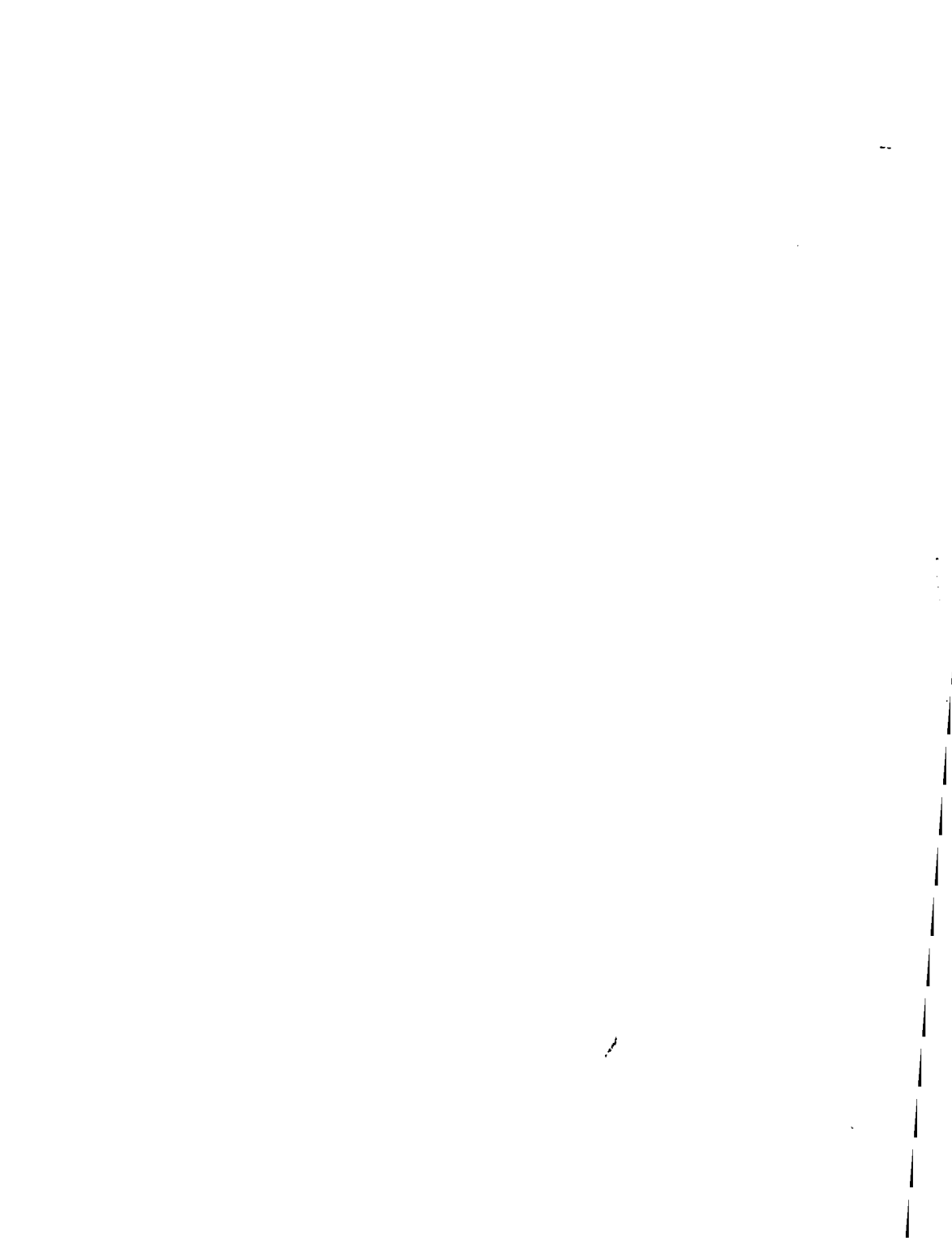


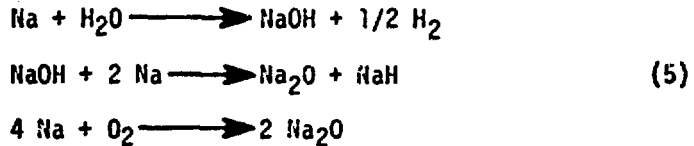
TABLE I. CALCULATED AND MEASURED LEAK RATES COMPARED

Condition	Crack Length inches	Pressure psig	Temperature, °F	Calculated	Leak Rate, g/hr Measured (Maximum)	<u>Measured</u> <u>Calculated</u>
1	0.5	150	746	24	107	4.5
2	0.33	150	650	4	55	13.8
3	0.33	150	600	3.6	41	11.4
4	0.33	150	800	4.6	45	9.8
5	0.5	150	800	24	98	4.1
6	0.47	200	800	36	110	3.1
7	0.25	200	800	2.8	67	24
8	0.25	200	1050	4.4	27.7	6.2

of flow. The typical appearance of the sodium reaction products near a leak to nitrogen, 1% O₂, 1000 ppm H₂O gas is shown in Figure 1.

Chemical Aspects of Leaks

In a nitrogen-oxygen-water vapor environment the major reaction products which are expected to be formed are H₂, NaH, NaOH and Na₂O. The formation of these products is governed by the following equations:



These equations represent a complex system for which at best one can obtain some quantitative information under thermodynamic equilibrium. However, at the vicinity of the leak non-equilibrium conditions may prevail with chemical kinetic and mass transport rates governing the relative amount of each product formed. Since chemical kinetic data for these reactions is almost non-existent and since the mass transport of oxygen, water vapor, and sodium through the reaction products as they accumulate is very complex, a rigorous description of the chemical behavior of small leaks is not possible. Consequently, certain questions pertaining to small leak behavior remain unanswered. For example, it would be of interest to know, (temperature, gas, composition, and sodium leak rate) a protective oxide film is formed on the pipe surface.

Experimentally^(2,3), it is observed that the nature of the reaction products formed is significantly affected by the water vapor content in the 100 to 6000 vppm range. At 6000 vppm H₂O, the leaking 800°F sodium reacts quickly to form a black liquid, which is presumed to be sodium hydroxide colored by dissolved or particulate corrosion products, e.g., NaFeO₂, NaCrO₂, etc.

At lower moisture levels (<1300 vppm) in the gas, whitish reaction products form initially (Na₂O(?)) which turn yellowish and brownish in time again perhaps due to the gradual accumulation of steel corrosion products. The reaction mass is much less fluid in this case.

At higher temperatures (1050°F), the tendency is to form black liquid even at 1000 vppm H₂O, for leak rates around 10 g/hr.

Corrosion Aspects of Sodium Leaks

Three types of corrosion mechanisms are of interest in the evaluation of potential damage which could result from small sodium to gas leaks:

- (a) General material wastage by metal reaction with the sodium/gas reaction products.

- (b) Stress corrosion cracking.
- (c) Corrosion enhanced fatigue.

(a) Material Wastage

At temperatures below 1000°F the corrosion rate of stainless steels in flowing sodium is⁽⁷⁾ less than 0.0002 in. per year per ppm O₂ concentration in the sodium. For sodium saturated with oxygen at 1000°F this corresponds to material wastage of 20 mpy. At the other extreme much more severe material wastage could result from NaOH attack on stainless steel. According to measurements⁽⁸⁾ conducted recently at Ohio State University, the corrosion rate of Type 304 stainless steel in fused sodium hydroxide varies from 90 to 640 mpy between 660 to 1000°F.

Experimentally^(2,3), general corrosion (metal loss), corrosion pitting, and intergranular attack has been observed. With 800°F sodium leaking to N₂, 1%O₂, 1300 vppm H₂O, general corrosion of 1 to 3x10⁻³ inches per month has been observed with the remaining surfaces exhibiting scattered pitting to a depth of 25x10⁻³ inches, and intergranular attack of 5 to 10x10⁻³ inches in 500 hour tests.

At 1050°F, with 1000 vppm H₂O, corrosion grooves to 60x10⁻³ inches were observed in a 500 hour test. This is a corrosion rate of 1036 mpy, which is similar to the corrosion rate of 304SS in pure sodium hydroxide quoted above. The general plus intergranular corrosion of about 10 mils per 500 hours at 800°F corresponds to about 173 mpy which is somewhat lower than the 253 mpy in sodium hydroxide which would be predicted from the Ohio State University data assuming the usual exp^{- (A/T)} temperature dependence. The general conclusion is that corrosion in a leaking sodium environment is severe -- approximating that in sodium hydroxide -- but piping integrity is nevertheless maintained for months even under these circumstances.

As already mentioned above, in the design of leak detection systems it is important to know the smallest leak that must be detected. In studying leak behavior, therefore, it is of interest to determine the smallest leak below which corrosion attack is confined to the immediate vicinity of leak. In this case corrosion will cause a gradual increase in the leak rate but will not damage the pipe to a degree where a sudden massive spill could occur. We proceed next to determine the size of such a leak.

The corrosion of metals in acids and in sodium is governed under many conditions^(9,10) by the diffusion of the dissolving metal atoms away from the metal surface. The driving force for the transport of these particles is the difference between the solubility C₀ of the dissolving metal in the liquid and the concentration of the metal in the bulk liquid, C_b. If R is the corrosion rate per unit area and D is the diffusion coefficient of the metal in the liquid we have:

$$\bar{R} = \frac{\bar{D}}{\delta} [C_s^0 - C_b] \quad (6)$$

where δ is the distance in the liquid which presents the main resistance to metal transfer. The enrichment with time of a volume V of liquid with the dissolving metal is given by:

$$V \frac{dc_b}{dt} = \bar{R}A \quad (7)$$

where A is the contact area between the metal and the dissolving liquid. Elimination of \bar{R} between Equations 6 and 7 yields the following expression for the increase in enrichment of the liquid with time.

$$\frac{C_s^0 - C_b}{C_s^0 - C_b^i} = e^{-\frac{\bar{D}t}{\delta^2}} \quad (8)$$

Here it was assumed that δ also equals the thickness of the liquid. This is true for either stagnant or very slow flowing systems. Equation 8 indicates that when:

$$\frac{\bar{D}t}{\delta^2} \rightarrow \infty \quad (9)$$

the bulk concentration C_b of the liquid approaches the solubility limit C_s^0 . In practice it is sufficient to replace ∞ by some constant, for example when:

$$\frac{\bar{D}t}{\delta^2} = 5 \quad (10)$$

the liquid will become more than 99% saturated with corrosion products. Next we examine a thin liquid film of constant thickness, which flows by gravity along a vertical wall. Such films may originate from small sodium leaks in the following manner: Upon reaching the crack exit, the sodium forms a drop approximately 0.5 cm in diameter which adheres to the pipe surface for a short period of time and then it bursts forming a liquid sheet of sodium hydroxide approximately 1 cm wide, which freely flows by gravity along the pipe wall. The average velocity of this film is given by the Equation⁽¹¹⁾:

$$\bar{U} = \frac{g\delta^2}{3\nu} \quad (11)$$

where ν is the kinematic viscosity of the liquid. The travel time t over a distance R along the wall is simply $\frac{R}{\bar{U}}$:

$$t = \frac{3Rv}{3\delta^2} \quad (12)$$

The elimination of the time t between Equations 10 and 12 gives a liquid film thickness which is completely saturated with corrosion products:

$$\delta = \left[\frac{3}{5} \frac{R \bar{D} v}{g} \right]^{1/4} \quad (13)$$

The corresponding mass flow of the saturated liquid is given by:

$$m = \rho \bar{U} \delta = \rho \frac{g}{3v} \left[\frac{3}{5} \frac{\bar{D} R v}{g} \right]^{3/4} \quad (14)$$

If R is equivalent to the pipe radius then Equation 11 represents a sodium leak rate for which the corrosion attack on the pipe will be limited to one radius distance from the leak origin. The liquid from smaller leaks will saturate at smaller than R distances from the leak origin thus reducing the potential for corrosion damage on surfaces far removed from the leak. Using the following representative numerical values, $\bar{D} = 1.5 \times 10^{-4}$ cm²/sec*, $R = 30$ cm, $v = 3.3 \times 10^{-3}$ cm²/sec, $\rho \sim 0.8$ g/cm³ we get a leak rate of approximately 265 $\frac{g}{hr-cm}$. Allowing one order of magnitude uncertainty in the diffusion coefficient we conclude that leaks of less than 30 $\frac{g}{hr-cm}$ will not corrode the pipe at distances larger than one radius from the leak. It should be noted that since a concentration gradient exists across the film the use of the entire film thickness δ in equation 6 instead of a smaller film thickness leads to conservative estimates of the minimum leak rate that will confine the corrosion damage to a distance of less than one radius from the leak.

When the leak originates on the top of a horizontal pipe equation 11 must be multiplied by $\cos \beta$ to account for the variations in the gravitational force as the film flows around the pipe, with β varying from 0 to 90°. Taking the average value of $\beta = 45^\circ$ Equation 14 needs to be multiplied by $(\cos 45) \frac{1}{4} \sim 0.92$ which does not significantly alter the results which were obtained for the vertical pipe.

(b) Stress Corrosion

Failures of austenitic steels in caustic environment has been observed on many occasions⁽¹¹⁾. Cracks are primarily transgranular and are formed at stresses which are below the yield strength of the material. In the Na-NaOH system the time to failure decreases with the decrease in concentration of sodium hydroxide in sodium. The time for the formation of cracks at 850°F is on the order of 14 to 30 days and crack propagation rates are as high as 1/4 in/hr⁽¹²⁾. Rigorous methods for predicting stress corrosion cracking in caustic environments do not exist. Stress corrosion cracking for a wide range of conditions in the presence of small leaks has not been observed.

*calculated from the Stokes-Einstein relation $\bar{D} = kT/6\pi\eta r$

In the Westinghouse, ARD experiments^(2,3) no evidence of stress corrosion cracking has been observed due to leaking sodium at 800°F and 1050°F in N₂, 1%O₂, H₂O < 6000 vppm. No cracks lengthened during the typical 500 hours test time, and no cracking on the pipe surfaces was observed; as noted above, however, there was considerable intergranular attack to 10 mils depth. The specimens were under stresses due to internal pressure (~200 psig in 12" OD, 0.375" thick pipe), and contained welded areas with their typical residual stress. Also, the stresses at the crack tips were enhanced of course.

(c) Corrosion-Enhanced Fatigue

The techniques of linear-elastic fracture mechanics have been shown to be quite useful in estimating the extension of cracks or flaws in reactor piping components due to the action of cyclic loadings encountered in service⁽¹³⁾. A variety of expressions relating the fatigue-crack growth rate (da/dN) in terms of the stress intensity factor (K) have been employed, but one of the simplest and most widely used is the power law due to Paris⁽¹⁴⁾.

$$\frac{da}{dN} = C (\Delta K)^n \tag{15}$$

where the stress intensity factor range (ΔK) is a function of both the stress field and the crack size. The values of C and n are generally determined experimentally and are dependent, in varying degrees⁽¹⁵⁾, upon the material, temperature, cyclic frequency, stress ratio, and the surrounding environment. In general, at a given level of ΔK , the crack growth rate can be thought of as being comprised of three components: one due to the mechanical fatigue process, one accounting for possible crack extension due to creep processes, and one accounting for crack extension due to the surrounding environment. Such an expression might be of the form:

$$\left. \frac{da}{dt} \right|_{total} = f \times \left. \frac{da}{dN} \right|_{fatigue} + \left. \frac{da}{dt} \right|_{creep} + \left. \frac{da}{dt} \right|_{environ.} = F(K) \tag{16}$$

In this case the fatigue-crack growth rate (da/dN) has been converted to a time-base crack growth rate (da/dt) by multiplying by the cyclic frequency (f). A similar superposition model involving two components, fatigue and environment, has been developed by Wei and Landes⁽¹⁶⁾.

It has been shown that a sodium environment, such as employed in an LMFBR, can have a significant influence upon the fatigue-crack growth behavior of austenitic stainless steels^(4,17). These studies have shown that fatigue-crack growth rates in a sodium environment at elevated temperatures are significantly lower than those in an air environment at the same temperature, and in fact, are approximately equal to crack growth rates observed at room temperature. Hence, one might expect that for cracks surrounded by a pure sodium environment, the environmental term in Equation (16) would be negligible. Similarly, it has been suggested⁽¹⁸⁾ that at the operating temperatures of LMFBR piping systems, the creep contribution

to crack extension may also be negligible. Therefore, for this case Equation (16) is equivalent to Equation (15). However, for the case of through the wall cracks which are exposed to an aggressive environment (e.g., sodium hydroxide), the environmental term in Equation (16) could possibly become quite significant.

To address this concern the sodium leak test program^(1,2) at Westinghouse ARD has been expanded to include an investigation of the effect of sodium leak environment on fatigue crack growth. An apparatus has been devised for cyclically flexing four inch diameter straight pipe sections, containing sodium and in which starter fatigue cracks have been formed. The rate of crack growth is to be measured continuously using a newly developed ultrasonic technique. By comparing da/dN values with a sodium leak, in pure nitrogen and at a variety of conditions, it will be possible to calculate the sodium environmental effect by means of Equation 16.

If, prior to reactor operation, the possibility of all through-wall cracks greater than a certain length ($2a_0$) has been eliminated by inspection, the initial crack size for sodium leaks will be less than $2a_0$. After a certain time (t) of reactor operation wherein the pipe is subjected to cyclic loadings, the half-crack length is given by integrating Eq. (16)

$$a = a_0 + \Delta a \quad \text{Eq. (17)}$$

$$= a_0 + \int_0^t F(K) dt$$

From Equation 4, the mass leak rate per unit crack length (m) is

$$\frac{m}{\rho} = \frac{\pi}{8} \cdot \frac{a^3 D^3 \Delta P^4}{\mu E^3 t^4} \quad (18)$$

with ρ = sodium density.

From our previous estimate that leaks less than 30 g/hr-cm pose no problems relative to extensive grooving corrosion (see also the following section) we can estimate that through wall cracks as large as $2a = 0.661$ cm length can be tolerated. Thus

$$a_0 + \int_0^t F(K) dt \leq 0.331 \quad (19)$$

gives the time before crack growth due to fatigue becomes a problem.

Equation (19) contains the assumption that the liquid flows uniformly along the length of the crack. Actually, for very slow leaks, experiments show that the sodium leaves the crack in the form of single drops. These drops which are approximately 0.5 cm in size, burst and form a liquid sheet of approximately 1 cm which falls by gravity along the wall. Equation (19)

should therefore be multiplied by some factor α which takes into account crack length, crack orientation, and the deviation of flow uniformity along the wall.

In the preceding discussion, it has been assumed that an initial through-wall crack of length $2a_0$ existed prior to the start of reactor service. It is, of course, far more likely that initial cracks if they existed at all, would penetrate only a small percentage of the piping wall thickness rather than the full thickness. It would therefore be necessary for such part-through cracks to penetrate the wall before a leak could develop. The prediction of such crack extension would be accomplished by integrating Equation (16), and an example of this procedure is shown in Reference 13. The half-crack length at wall penetration could then be used in place of a_0 in Equation 19, and the time for penetration added to the time calculated by Equation 19.

Instrument Response for Leak Detection

The foregoing discussion of leak size, crack propagation and material wastage leads to the question how all this information impacts the minimum time which is required to detect a sodium leak. It has been estimated that sodium leaks greater than 10,000 gallons per minute must occur before plant safety is compromised. Such a massive spill can occur only when the crack, as described by Equation 17 reaches some critical size a_{cr} or when the pipe wall is corroded to sufficient depth over a significant length of the pipe circumference. In the first case this time is given by:

$$t_{cr} = \int_{a_m}^{a_{cr}} \frac{da}{F(K)} \quad (20)$$

The time to detect a leak must be considerably less than t_{cr} to allow for instrument checkout and for ordinary plant shutdown. Thus:

$$t_d \ll t_{cr} \quad (18)$$

Currently it is estimated that cracks will not grow measurably in the lifetime of the plant, based on fracture mechanics analysis, hence Equation 18 is not a controlling criterion.

In the second case, when corrosion resulting from the leak is more rapid than the original crack propagation rate the time to detect a leak will be given by:

$$t_D = \frac{\ell - \Delta}{R} \quad (18)$$

max.

where:

ℓ = actual wall thickness
 Δ = minimum wall thickness required for combined pipe loading

$R_{\max.}$ = maximum corrosion rate.

Δ must be determined from stress analysis and one would expect large variations to exist. For the simple case of pressure loading on a pipe alone, and assuming that Δ is the thickness at which the stress becomes equal to the yield stress, σ_y , we have:

$$\sigma_y = \frac{PD}{2\Delta}$$

or

$$t_D = \frac{\ell - \frac{PD}{2\sigma_y}}{R_{\max.}}$$

For CRBR cold leg conditions ($P = 200$ psig, $\ell = 0.375$ " , $D = 24$ " , $\sigma_y = 17,000$ psi, $R_{\max.} = 2.75 \times 10^{-6}$ in/hr* (23.8 mpy)) $t_D = 85026$ hours or 9.7 years. Even if we use the worst observed corrosion rate 1036 mpy; t_D equals 0.226 years or 82 days.

It is apparent from the above that speed of response is not a controlling factor in the selection of leak detection systems. With regard to size of leak, it was previously shown that leaks smaller than 30 g/hr cannot lead to critical failures. In conjunction with the above analysis, it can be concluded that small leaks will only be enlarged after about 82 days of leakage and they will enlarge gradually.

In actual practice, of course, any leak detector based on vapor or aerosol analysis, or radioactivity analysis can be expected to respond in almost a day or so since circulation, purification, plate-out and radioactive decay would all have kinetics which would lead to steady state conditions in a few days at most. Therefore, a detector which can detect about 30 g/hr leakage in a few days would be more than satisfactory to protect against all leaks, assuming such leaks are originating and growing by corrosion.

For leaks larger than 30 g/hr, if they were to occur, response time of leak detectors is on the order of several hours thus preventing massive spills.

SUMMARY AND CONCLUSIONS

Although much experience on sodium to gas leaks has been accumulated from the operation of sodium loops and sodium cooled reactors a concern was raised several years ago that the information regarding leak behavior and leak detection requirements was still not sufficient. In response, ERDA initiated studies on sodium flow characteristics through small pipe cracks, corrosion damage from sodium leaks, fatigue and propagation with and without the presence of sodium leaks, and sensitivity and reliability of

*Evaluated from Equation 6 using $C_S = 1$ ppm, $C=0$.

various leak detection instruments. While not all of the above studies have yet been completed the results obtained to date allow a theoretical and practical analysis of sodium to gas leaks.

Sodium leaking from pipe cracks reacts with water vapor and oxygen contaminants from the surrounding atmosphere. The reaction products in contact with the pipe wall induce corrosion and ultimately will result in larger sodium leaks. However, it was shown in this paper that leaks smaller than 30 g/hr-cm will limit the corrosive attack to the immediate vicinity of leak thus precluding the possibility of a massive sodium spill which would follow a guillotine-type pipe rupture. These conclusions are born out to some extent by field experience, where numerous sodium leaks have occurred without resulting in a guillotine-type pipe rupture. State-of-the-art leak detectors are capable of detecting leaks of 10 g/hr and larger without giving spurious signals.

Information on the effect of sodium leak environment on fatigue crack growth is still lacking. The on-going programs at HEDL and WARD will fill this gap and thus provide further support for the definition of sodium to gas leak detection requirements.

REFERENCES

1. "Guide for Economic Evaluation of Nuclear Reactor Plant Designs," NUS-581, January 1969.
2. W. L. Matheys, Sodium Leak Characterization Test, WARD-LT-3045-1, February 1975.
3. W. L. Matheys, Sodium Leak Characterization Test, WARD-LT-3045-2, February 1976.
4. L. A. James and R. L. Knecht, "Fatigue-Crack Propagation Behavior of Type 304 Stainless Steel in a Liquid Sodium Environment," Metallurgical Transactions, Vol. 6A, No. 1, pp. 109-116 (1975).
5. H. L. Dryden, F. D. Murnaghan, and H. Bateman, Hydrodynamics, pp. 181 ff. Dover Publications Inc., 1956.
6. R. G. Forman, "Effect of Plastic Deformation on the Strain Energy Release Rate in a Centrally Notched Plate Subjected to Uniaxial Tension," Trans, ASME, p. 82ff, March 1966.
7. C. Bagnall and D. C. Jacobs, "Relationships for Corrosion of Type 316 Stainless Steel in Liquid Sodium," WARD-NA-3045-23, May 1975.
8. F. Du, "The Corrosion of Iron Nickel, Chrome Alloys in Fused NaOH" Unpublished MS Thesis Department of Metallurgical Engineers, Ohio State University.

9. V. G. Levich, "Physiochemical Hydrodynamics", Prentice-Hall, Inc., Englewood Cliffs, New Jersey, 1962, p. 337.
10. J. Hopenfeld, "Corrosion of Type 316 Stainless Steel with Surface Heat Flux in 1200°F Flowing Sodium," Nuclear Engineering and Design, 12, 167-179.
11. R. B. Bird, W. E. Stewart, and W. N. Lightfoot, Transport Phenomena, pp. 37 ff, John Wiley & Sons, Inc., November 1966.
12. G. C. Wheeler, "A Look at Caustic Stress Corrosion," POWER, September 1960, p. 86.
13. L. A. James, "Estimation of Crack Extension in a Piping Elbow Using Fracture Mechanics Techniques," Journal of Pressure Vessel Technology, Vol. 96, No. 4, pp. 273-278 (1974).
14. P. Paris and F. Erdogan, "A Critical Analysis of Crack Propagation Laws," Journal of Basic Engineering, Vol. 85, No. 4, pp. 528-534 (1963).
15. L. A. James, "Fatigue-Crack Propagation in Austenitic Stainless Steels," Atomic Energy Review, in press.
16. R. P. Wei and J. D. Landes, "Correlation Between Sustained-Load and Fatigue Crack Growth in High-Strength Steels," Materials Research and Standards, Vol. 9, No. 7, pp. 25-27, 44, 46 (1969).
17. E. K. Priddle and C. Wiltshire, "The Measurement of Fatigue Crack Propagation in Specimens Immersed in Liquid Sodium at Elevated Temperatures: Technique and Preliminary Results," International Journal of Fracture, Vol. 11, No. 4, pp. 697-700 (1975).
18. L. A. James, "Some Questions Regarding the Interaction of Creep and Fatigue," Journal of Engineering Materials and Technology, in press, (ASME Paper 75-WA/Mat-6).